https://doi.org/10.5194/egusphere-2022-767
Preprint. Discussion started: 16 August 2022

Determination of NO_x emission rates of sailing inland ships from on-shore measurements

Kai Krause[1], Folkard Wittrock[1], Andreas Richter[1], Dieter Busch[2], Anton Bergen[2], and John P. Burrows[1]

[1]Institute of Environmental Physics, University of Bremen, Bremen, Germany
[2]State Agency for Nature, Environment and Consumer Protection in North Rhine-Westphalia (LANUV NRW), Recklinghausen, Germany

Correspondence: Kai Krause (kakrau@iup.physik.uni-bremen.de)

Abstract. Inland ships are an important source of NO_x, especially for cities along busy waterways. The amount and effect of these emissions depends on the traffic density and the NO_x emission rates of the individual vessels. Monitoring of ship emissions is usually carried out using in situ instruments on land and often relative NO_x emission factors, e.g. the amount of emitted pollutants per amount of burnt fuel is reported, but in this study, NO_x emission rates in $\mathrm{g\,s^{-1}}$ are investigated. Within the EU Life project Clean Inland Shipping (CLINSH), a new approach to calculate NO_x emission rates from data of in situ measurement stations has been developed and is presented in this study. Peaks (i.e. elevated concentrations) of NO_x were assigned to the corresponding source ships and each ship passage was simulated using a Gaussian-puff-model in order to derive the emission rate. In total over 32900 ship passages have been monitored over the course of 4 years. The emission rates of NO_x were investigated with respect to ship speed, ship size and direction of travel. Individual comparisons of the on-shore emission rates and those made on-board of selected CLINSH ships show good agreement. Also the emission rates are of similar magnitude as emission factors from previous studies. In contrast to relative emission factors (in grams per kilogram fuel), the emission rates (in grams per second) do not need further knowledge about the fuel consumption of the ship and can therefore be used directly to investigate the effect of ship traffic on air quality.

1 Introduction

In cities along busy waterways such as the Rhine, the diesel engines of inland vessels are a significant source of emissions of pollutants (i.e. oxides of nitrogen (NO_x), sulphur dioxide (SO_2), carbon monoxide (CO), and aerosols). The total amount and effect of these emissions depends on the traffic density along those waterways and the emissions of the individual vessels. In order to limit the effects of these emissions on air quality, the Central Commission for Navigation on the Rhine (CCNR) and the EU have established, during past decades, regulations for ship engines (EUD, 1998; EUR, 2016; CCNR, 2020). However, these regulations only apply to new engines (new ship construction or replacement of old engines). Engines on ships already in service are subject to grandfathering and do not have to comply with newer regulations. The effect of these requirements is therefore limited, as ship engines have a long service life. There is no provision for continuous monitoring of emissions from ships in service, as is the case with road vehicles, for example. To determine the emissions of shipping traffic, there has been a lack of measurements of both the shipping traffic and the emissions from the different types of ship engines during real cruising

https://doi.org/10.5194/egusphere-2022-767
Preprint. Discussion started: 16 August 2022

operation. Consequently, a large number of assumptions had to be made in order to determine the mean emissions caused by the ships.

There are several studies, which investigated ship emissions and derive emission factors for short time periods or for specific ships, but there is a lack of long time observations, especially for inland ships. Shipping emission have been typically investigated using in situ instruments, either on-board or on-shore (e.g., Moldanová et al., 2009; Alföldy et al., 2013; Diesch et al., 2013; Beecken et al., 2014; Pirjola et al., 2014; Beecken et al., 2015; Kattner et al., 2015; Kurtenbach et al., 2016; Kattner, 2019; Ausmeel et al., 2019; Celik et al., 2020; Walden et al., 2021). Additionally, remote sensing techniques such as differential optical absorption spectroscopy (DOAS) (e.g., Berg et al., 2012; Seyler et al., 2017, 2019; Cheng et al., 2019; Krause et al., 2021) and more recently UAVs are used to investigate ship emissions (Zhou et al., 2019, 2020). The long term impact of shipping emissions has been investigated by modelling studies (Eyring et al., 2005; Ramacher et al., 2018, 2020; Tang et al., 2020; Wang et al., 2021; Jiang et al., 2021).

Within the EU Life Project Clean Inland Shipping (CLINSH), two methods to measure ship emissions were used. In-situ instruments on-board of ships were deployed to measure the emissions of the engines directly at the exhaust. Measurements were carried out on 40 inland vessels, which participated in the project. Absolute NO_x emission rates (in $\mathrm{g\,s^{-1}}$) have been derived from these measurements. In addition, a method to derive absolute NO_x emission rates from on-shore measurements has been developed and is presented in this study. The retrieval concept builds on the approach presented in Krause et al. (2021), but the method has been improved and the algorithm can now be used with data measured by any standardized in-situ measurement station located in the vicinity of a river.

In total more than 32900 ship passages have been identified and analysed between 2017 and 2021 and provide a data set, which will be used in the future update of the inland waterway vessel emission register of the state of North Rhine-Westphalia. In contrast to more regularly reported emission factors in $\mathrm{g\,kg^{-1}}$ or $\mathrm{g\,kWh^{-1}}$, the derived NO_x emission rates may be used directly without further assumptions regarding the fuel consumption of the ships and directly reflect the real driving conditions at this part of the Rhine.

2 Measurement sites

For the CLINSH project, the State Agency for Nature, Environment and Consumer Protection in North Rhine-Westphalia (LANUV NRW) set up continuous measurement stations in Duisburg and in Neuss, which measure NO_x concentration and meteorological parameters such as atmospheric pressure, humidity, temperature, wind speed and wind direction close to the river Rhine. The on-shore measurements were carried out using standardized air quality monitoring stations. NO and NO_2 are measured using the chemiluminescence method, wind speed is measured by a rotary anemometer and wind direction by a wind vane. NO_x is then calculated as the sum of NO and NO_2. The temporal resolution of those measurements is five seconds. Additionally, the measurement stations also are supplemented with AIS (automatic identification system) receivers, which deliver information about the passing ships. Under favourable wind conditions (wind blowing ship plumes towards the in situ

https://doi.org/10.5194/egusphere-2022-767
Preprint. Discussion started: 16 August 2022

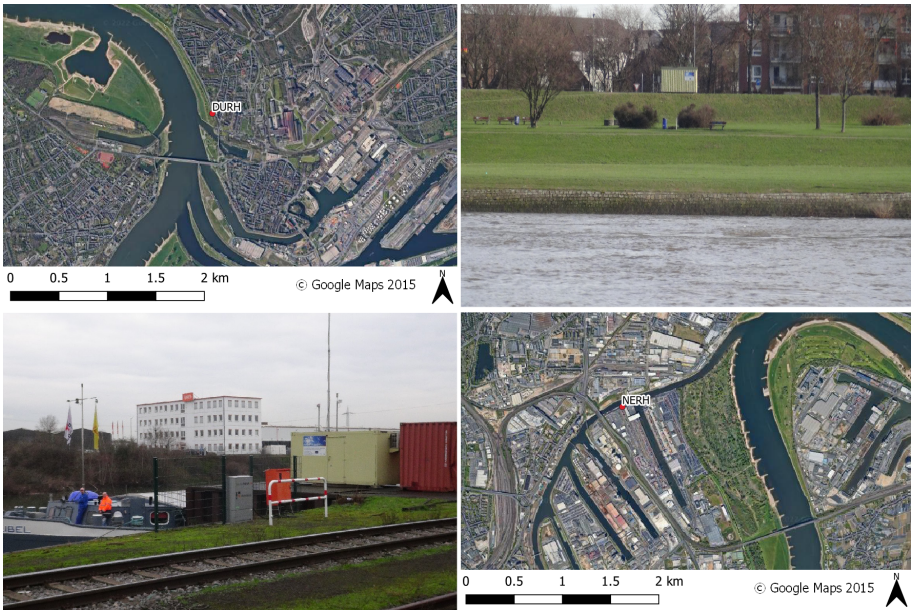

Figure 1. Views of the two different measurement sites used in this study. The upper row shows a satellite image of the DURH station and a picture of the measurement container as seen from the Rhine. The lower row shows a picture of the measurement container in the NERH and a satellite picture of its location.

systems), both measurement stations show strong enhancements of NO_x when ships pass the measurement site, which can be clearly seen as a peak in the time series. Different views of the measurement sites are shown in Figure 1.

2.1 Duisburg Rhine Harbour (DURH)

In Duisburg, the measurement site is located on the eastern riverbank of the Rhine. As the predominant wind direction has a westerly component, emissions from ships are transported towards the measurement site for the majority of the time. Consequently a large number of pollution peaks from ships passing are identified in the measured NO_x concentration time series (e.g. Figure 2). Generally, this measurement site is well located to derive NO_x emission rates from ships sailing along the Rhine, because it is close to the Rhine and the entrance to the Duisburg harbour basins. Consequently, the measured concentration peaks can be differentiated for ships that pass the measurement site in different driving conditions e.g., ships that drive upstream against the river current or downstream with the river current. This measurement station has been set up in October 2017 and is still active at the time of writing. In this study, measurements from 2017 until the end of 2021 are evaluated.

2.2 Neuss Rhine Harbour (NERH)

In contrast to the measurement site DURH, the measurement site in Neuss is located within the Neuss harbour on the west side of the Rhine. Buildings and vegetation block the direct line of sight from the measurement station to the Rhine. The

https://doi.org/10.5194/egusphere-2022-767
Preprint. Discussion started: 16 August 2022

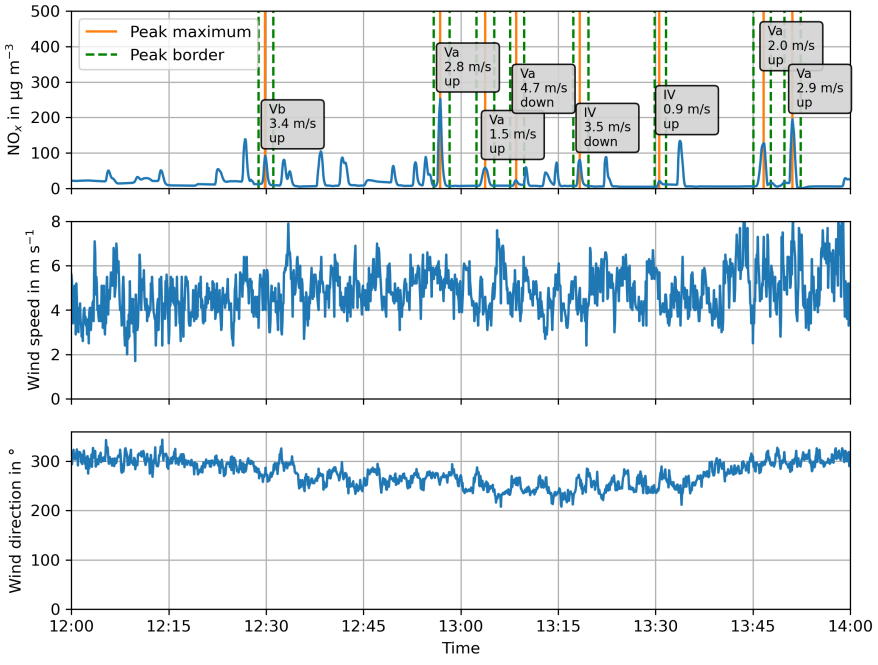

Figure 2. Example of the measured NO_x concentration, wind speed and wind direction at DURH. Ship peaks identified in the NO_x concentration are marked with an orange line, their borders are green dashed lines. The text box at each peak shows the ship class, the speed over ground and the direction of travel. Peaks without a label are most likely also caused by passing ships, but in these cases, unambiguous assignment of a source was not possible.

combination of its location and the predominant south-westerly wind direction leads to only a few plumes being detected at this measurement site from ships that are steaming along the Rhine. Nevertheless, due to its location directly within the harbour, this measurement site is well suited to evaluate the emissions of slow moving ships within the harbour area where the influence of the river currents on engine operation are negligible. This measurement station was set up in September 2017 and dismantled at the end of 2019. Therefore, NO_x emission rates could be derived for the years 2017 to 2019.

3 Methods

Combining the measurements of NO_x and the received AIS signals enables ship emissions from passing ship to be calculated. The approach uses three consecutive steps, which are described in the following.

3.1 Peak identification

The first step is to identify the peaks of NO_x caused by passing ships. To identify these peaks, a low pass filtered time series is calculated from the measured time series using a running median with a window length of 5 minutes. This low pass time

https://doi.org/10.5194/egusphere-2022-767
Preprint. Discussion started: 16 August 2022

series describes the changes in the background concentration caused by meteorological factors and other emission sources, but excludes the short-term variation caused by passing ships. The low pass filtered time series is then subtracted from the measured time series, resulting in a time series, which is close to zero on average, but still shows the sharp peaks caused by the passing ships. This time series is then analysed. If the NO_x peaks exceed a defined threshold then it is defined as an NO_x plume from shipping. The threshold is selected to ensure that the peaks are enhancement of NO_x, caused by shipping emissions and not noise in the measurements. In this case, the threshold was defined as 2 ppbv. For each identified peak, the time of occurrence (t_{peak}), the peak width, and the height of the maximum above the background concentration are determined.

3.2 Ship assignment

The second step is to identify the respective source of the peak. For each peak, all ships within a 5 km radius around the measurement site up to 5 minutes before the peak maximum were investigated. For each ship, the corresponding AIS signals within the given time frame are collected and interpolated to a one second time resolution. For each AIS signal position, a trajectory is calculated to assess whether emissions caused at that specific ship position could have been transported to the measurement site by the wind. The wind speed and direction used for these trajectories are the 30 min averages of wind speed and wind direction at the measurement site. Each trajectory is calculated for the period between the time stamp of the AIS signal (t_{AIS}) and the time of the peak maximum (t_{peak}). It is then checked, whether the trajectory ends within a 50 m radius of the measurement site. If only the trajectories of a single ship end close to the measurement site in the selected time window, then this ship is assigned to be the source of the NO_x peak.

For cases, where several ships are identified as possible sources of the peak, these peaks are not analysed further, because unambiguous assignment of a single ship, as the source of the NO_x emission, is not feasible. Once a ship has been identified as the source of the NO_x peak, the relevant information (e.g. position, course and speed) for that particular ship passage is assigned to the peak. The first assigned ship position is the position transmitted 180 seconds before t_{AIS} and the last assigned position is the position 180 seconds after t_{peak}. The section of these start and end points ensures that the entire NO_x emission plume form a particular ship, during its passage across the measurement site, is recorded.

3.3 Calculation of emission rate

In the third step, the NO_x emission rate for each peak assigned to a source ship is calculated. As the stations only measure the concentration of NO_x at the measurement site and not at the stack of the ship, a model has to be applied to estimate the emission rate from the concentration enhancement found at the measurement site. The method, which we have chosen, is to assume that the plume of the ships can be described by a Gaussian-puff-model (Zenger, 1998):

$$C(x,y,z) = \sum_{i=1}^{N} \frac{Qdt}{\sigma_x \sigma_y \sigma_z (2\pi)^{1.5}} \cdot \exp\left(\frac{-(x - U\cdot(t-dt))^2}{2\sigma_x^2}\right) \cdot \exp\left(\frac{-y^2}{2\sigma_y^2}\right) \cdot \left[exp\left(\frac{-(z-H)^2}{2\sigma_z^2}\right) + exp\left(\frac{-(z+H)^2}{2\sigma_z^2}\right)\right] \quad (1)$$

where the concentration at a point ($C(x,y,z)$) is assumed to be a function of the emission rate (Q), the dispersion due to atmospheric stability (σ_x, σ_y, σ_z), the length of time of the emission (dt) at a certain source point (x=0, y=0), funnel height

https://doi.org/10.5194/egusphere-2022-767
Preprint. Discussion started: 16 August 2022

(H), the total transport time (t) and the wind speed (U). The wind direction is taken to be along x. The model releases a puff of pollutants at the ship's position, which is then transported by the wind for an amount of time ($t - dt$) and dispersed according to the current atmospheric stability. The time (t) is different for each ship position and is always the time of the last AIS signal of the ship passage (t_{peak} + 180 seconds) minus the time of the respective AIS signal (t_{AIS}). The result is a concentration field caused by the emission of pollutants at the specific ship location for a time step dt. This procedure is then repeated for all ship positions. The calculated concentration fields then describe how the plume developed during the ship passage (e.g. Figure 3).

As the emission rate is unknown, the model is run with an arbitrary but constant emission rate (Q_{model}). The height of the plume centre is approximated to be at the height of the funnel above water level, assuming that the plume quickly bends down due to wind and movement of the ship. It is also assumed that this height is roughly the same for all ships. Dispersion parameters are chosen according to atmospheric stability, which has been determined using the wind speed at the measurement site and incoming global radiation (DWD Climate Data Center, a) during day and cloud coverage (DWD Climate Data Center, b) during night from a nearby weather station of the German Weather Service located at the Düsseldorf-Airport. To derive the emission rate, the integrated measured concentration, i.e. the area under the peak (C_{meas}), which has been corrected for the fluctuating background, is compared to the modelled concentration at the measurement site, i.e. the area under the modelled peak (C_{model}). Assuming the model sufficiently describes the ships plume, the only difference between modelled concentration and measured concentration is caused by the different emission rate. Consequently, the emission rate of the ship (Q_meas) is estimated by the following equation:

$$Q_{meas} = \frac{C_{meas}}{C_{model}} \cdot Q_{model} \tag{2}$$

This approach assumes, that the emission rate is constant for the whole modelled time domain. An example is shown in Figure 4.

3.4 Quality control

The assumptions made in the model to estimate the NO_x emission rate may not truly represent the conditions at the time of measurement. To assess the quality of the derived emission rate, Monte-Carlo-simulations are performed to assess whether a small change in one of the input parameters results in a large change of the derived concentration at the measurement site. The parameters varied are wind speed, wind direction, atmospheric stability and the position of the ship in longitude, latitude and height. Each of these parameters is changed within the uncertainty ranges given in Table 1. For each changed parameter, the derived integrated peak concentrations are then compared to the integrated peak concentration of the reference simulation. If the Monte-Carlo-simulations and the reference simulation do not show large deviations, the derived NO_x emission rates for that specific case are used for further evaluation.

https://doi.org/10.5194/egusphere-2022-767
Preprint. Discussion started: 16 August 2022

Table 1. Uncertainties of the input parameters used in the Monte-Carlo-Simulations.

Abbreviation	Name	Calculation of value
σ_{lon}	source position longitude	Uncertainty of the AIS signal, 10 m
σ_{lat}	source position latitude	Uncertainty of the AIS signal, 10 m
σ_H	plume height	$\sqrt{\sigma_{fh}^2 + \sigma_{wl}^2}$
σ_{fh}	funnel height	estimated: 5 m
σ_{wl}	water level	mean high water level - mean low water level
σ_U	wind speed	standard deviation of the wind speed
σ_θ	wind direction	estimated: 10 °
$\sigma_{stability}$	stability	atmospheric dispersion parameters of class with lower stability and higher stability than the assigned class
$\sigma_{c_{meas}}$	uncertainty of the measured peak area	$\sqrt{std(peak)^2 \cdot n}$, where n is the number of nodes used to calculate the peak area

3.5 Uncertainty of the NO_x emission rates

In this section we investigate the uncertainty of the measurement. This is considered to the standard error of the emission rate, i.e. one standard deviation of the distribution of emission rates. The uncertainty of the derived emission rate is given by:

$$\sigma_Q = \sqrt{\left(\frac{\partial Q_{meas}}{\partial C_{meas}} \cdot \sigma_{C\,meas}\right)^2 + \left(\frac{\partial Q_{meas}}{\partial C_{model}} \cdot \sigma_{C\,model}\right)^2} \tag{3}$$

where σ_{Cmeas} is the uncertainty of the measured integrated peak trace gas concentration and σ_{Cmodel} is the uncertainty of the modelled integrated peak trace gas concentration. The uncertainty of the model is defined as:

$$\sigma_{C\,model} = \sqrt{\sigma_{C\,U}^2 + \sigma_{C\,\theta}^2 + \sigma_{C\,stability}^2 + \sigma_{C\,lon}^2 + \sigma_{C\,lat}^2 + \sigma_{C\,H}^2} \tag{4}$$

where each σ_{Cj} is the standard deviation of the modelled trace gas concentrations of the Monte-Carlo-simulations with respect to changes of an individual input parameter (j).In the Monte-Carlo-simulations, each parameter is varied individually, i.e. independently. The consequences of the changes of more than one parameter at a time are assumed to be negligible.

4 Results

For Duisburg, a total of 32900 ship peaks has been identified and could be assigned to specific source ships. For 23500 of those peaks it was possible to determine the NO_x emission rate, which fulfil the quality criteria. In Neuss, 5500 peaks have been identified and the respective emission rates have been derived, in 3200 cases those derived NO_x emission rates fulfil the quality criteria. The number of identified ship plumes is mainly limited by the wind, as the wind is needed to transport the

https://doi.org/10.5194/egusphere-2022-767
Preprint. Discussion started: 16 August 2022

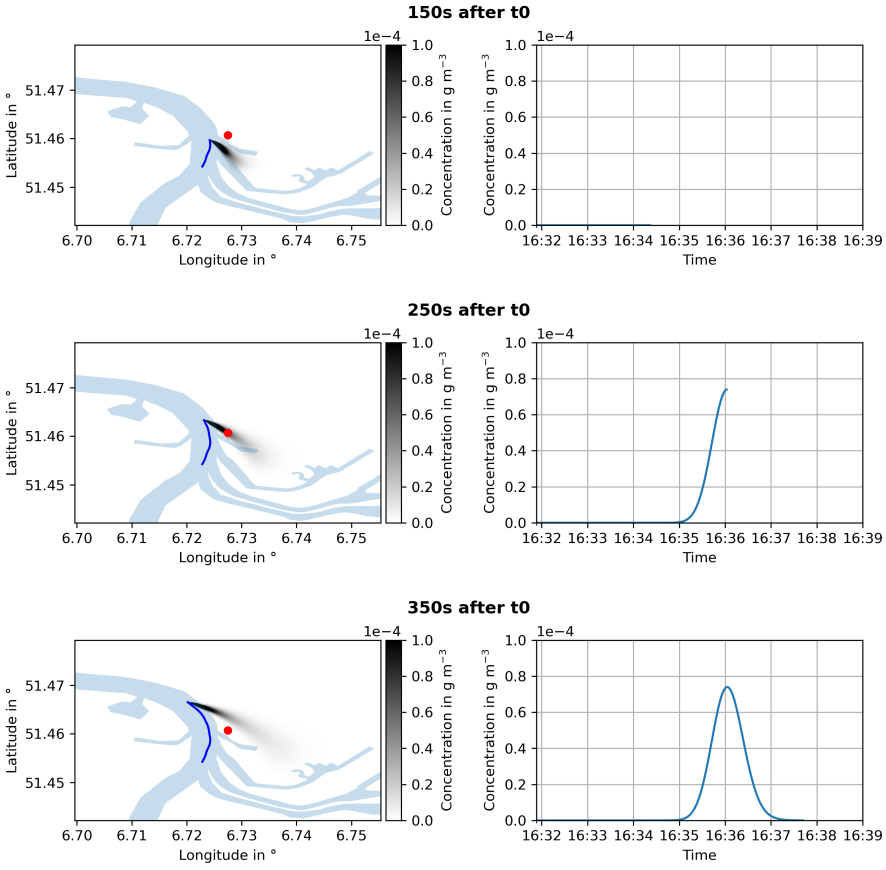

Figure 3. Example of a plume simulation for different time steps after the simulation start (t0). The upper, middle and lower panels show the movement of the modelled ship plume 150 s, 250 s and 350 s after the initiation of the plume. The left column shows a horizontal cross section of the modelled plume in 20 m height. The location of the measurement station is marked as a red dot. The blue line in the right column shows the modelled concentration at the location of the measurement station during the model run.

emitted pollutants towards the measurement site. An additional limitation is the traffic density as in situations of high traffic, an unambiguous identification of a ship plume is often not possible.

The derived emission rates were then summarized in the context of the respective CEMT ship class (Table 2), the direction of travel (upstream or downstream) and their speed over ground (e.g. Figure 5). The most common ship classes are IV, Va, Vb and Jowi, which together account for approximately 80 percent of the total ship traffic (Figure 6). Between 2017 and 2021, there were approximately 256 ship passages each day. As can be seen in Figure 7, the majority ships travelling upstream have a speed over ground of about 3 $\mathrm{m\,s^{-1}}$, while the majority of ships travelling downstream have speeds over ground of about 5 $\mathrm{m\,s^{-1}}$.

https://doi.org/10.5194/egusphere-2022-767
Preprint. Discussion started: 16 August 2022

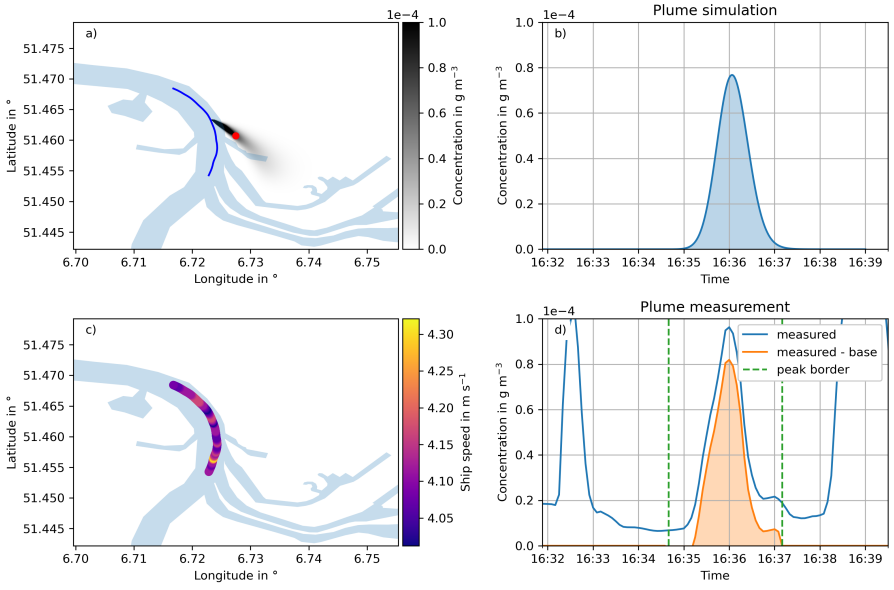

Figure 4. An example of a plume simulation for the 22nd August 2018 at 16:36 UTC compared with the measured plume. a) a map of the modelled plume for the time when the highest concentration has been measured. b) a plot of the simulated concentration of NO_x at the measurement site as a function of time. c) a map showing the ship speed over ground for each time step. d) a plot of the measured NO_x concentration as a function of time at the measurement station. The blue line represents the NO_x concentration, and the orange line is the background corrected NO_x concentration of the peak.

For the most common ship classes, this enables the NO_x emission rates of the respective class under real driving conditions to be characterized. For less common ship classes, there are fewer observations, which leads to a higher uncertainty of the summarized NO_x emission rates for these classes. In addition, there might not be enough data to differentiate sufficiently between direction of travel or different speeds.

The speed over ground is correlated with the emission rates, higher speeds leading to higher emissions as expected (e.g. Figure 8).

Furthermore, the direction of travel is important when investigating the emissions for a given speed. Ships that travel upstream have to overcome the river current and therefore need more power to achieve the same speeds over the ground compared to ships travelling downstream. With the same speed in water, the engine operating conditions should be similar and independent of direction of travel. Consequently, we assume that the NO_x emission rates are similar. A direct comparison for ship classes IV, Va, Vb and Jowi shows, that ships travelling upstream with a speed of about 3 $\mathrm{m\,s^{-1}}$ and ships travelling downstream with a speed of 5 $\mathrm{m\,s^{-1}}$ have similar NO_x emission rates in their respective size class (shown in Table 4), which suggests similar operating conditions. Ships that are not influenced by the current show similar NO_x emission rates independent of direction of travel (e.g. Figure 9).

https://doi.org/10.5194/egusphere-2022-767
Preprint. Discussion started: 16 August 2022

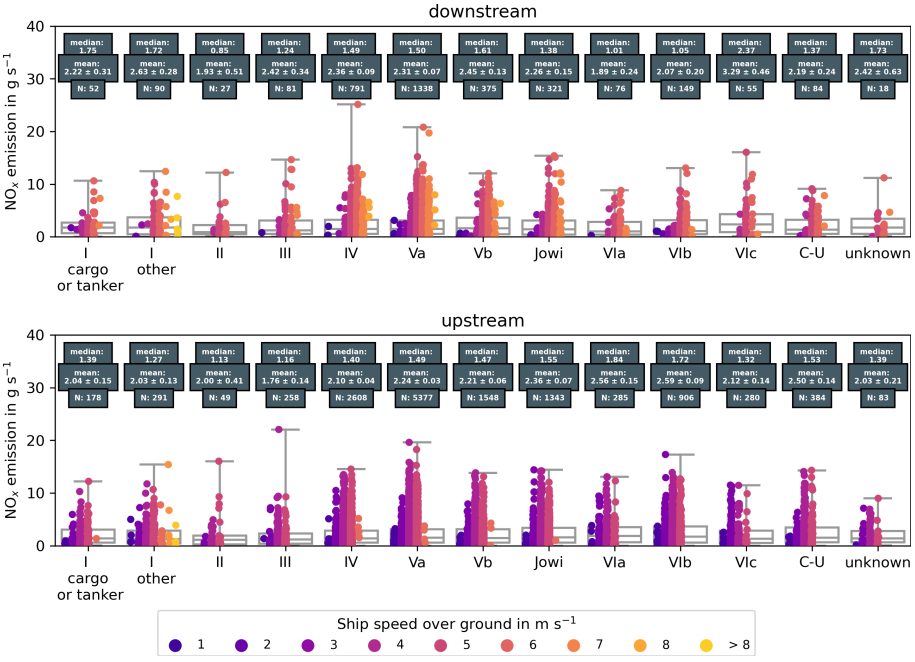

Figure 5. NO_x Emission rates for all ship classes, derived from measurements at DURH. Single measurements are colour-coded to the respective mean ship speed during the measurement.

Unfortunately, at the DURH station most of the identified ships are vessels which are travelling upstream. The main wind direction at DURH is south-west which is parallel to the river, and ship plumes are therefore transported along the river. Unambiguous assignment is only possible if there is just a single ship plume that can reach the measurement station. Ships travelling upstream need a longer time to pass through the area, as they are slower than ships travelling downstream. Therefore, in cases of high traffic density, the longer time window of the slower upstream travelling ships increases the chances of an unambiguous identification and results in a larger number of observed ship plumes for that particular direction.

The NO_x emission rates in the context of size are more difficult to summarize. Generally, larger ships show larger NO_x emission rates than smaller ships. At the same time, the larger ships are usually newer and their emissions are regulated, while older ships are subject to grandfathering, which means their engines do not have to comply with new regulations. Only if the engine of an older ship is exchanged, are the new regulations applicable. Due to the long service life of inland ships, a lot of the smaller ships do not fall under the regulations and therefore still have high emissions.

4.1 Comparison with on-board emissions measurements

In order to validate the emission factors within the CLINSH project, a comparison has been carried out between the values derived here from on-shore observations of the CLINSH fleet and the respective on-board measurements. CLINSH ships have been identified using the AIS signal as described in section 3. For the NO_x plumes from shipping, which passed the quality

https://doi.org/10.5194/egusphere-2022-767
Preprint. Discussion started: 16 August 2022

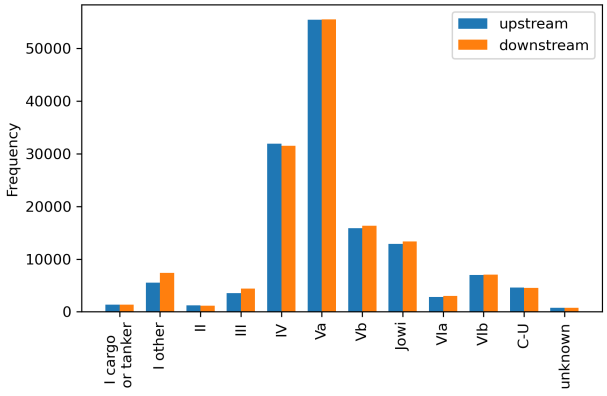

Figure 6. Ship traffic and fleet composition at DURH between November 2017 and December 2021. In total 291635 ship passages have been identified.

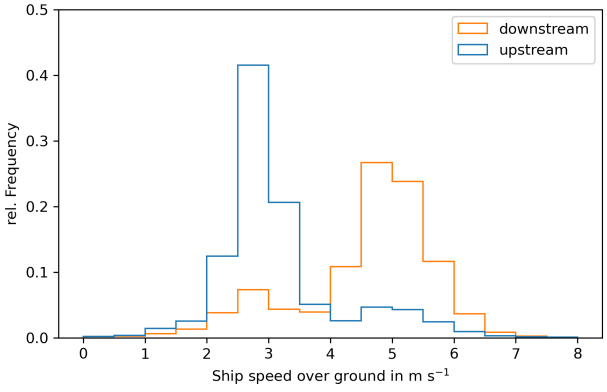

Figure 7. Ship speed over ground for all ship passages identified at DURH as a function of direction of travel.

control criteria, the CLINSH data was searched to identify whether on-board data are available for the same time interval. For the case of a match, on-board data have been averaged for the period, in which the plume detected by the on-shore observation system was released by the ship. As the uncertainty of the Gaussian-puff-model is quite high, data one minute before and after the release time were included in the plume average to take this into account. The 16 different CLINSH ships were observed nearly 200 times with both on-board and on-shore measurement systems. Table 3 and Figure 10 give a summary of the results obtained.

For almost half of the ships, the agreement between on-board and on-shore observations is good and well within the error bars. However, it turns out that for some ships (e.g. ship M), on-shore values are systematically higher than the on-board data for the same time. One possible explanation is that some ships use more than one main engine for navigation, but the on-board measurement systems usually only capture the emissions of one of the engines and not the total amount emitted at the stack.

https://doi.org/10.5194/egusphere-2022-767
Preprint. Discussion started: 16 August 2022

Table 2. Modified ship classification scheme based on CEMT (European Conference of Ministers of Transport, 1992) classes. Ships are categorized by their respective length and width, e.g. a ship longer than 86 m but shorter than 111 m and width between 10 and 12 m is classified as class Va. Additionally coupled units are identified via their Electronic Reporting International (ERI) code which is also transmitted in the AIS signals.

Class	maximum length	maximum width	cargo capacity
	m	m	tons
I	39	6	350
II	56	7	655
III	68	9	1000
IV	86	10	1350
Va	111	12	2750
Vb	136	12	4000
Jowi	136	18	5300
VIa	173	12	5500
VIb	194	23	11000
VIc	194	35	16500
Coupled unit (C-U)	motor freighter pushing one barge identified via ERI identifier		
unknown	ships without information about width and / or length		

The total emission rate for all main engines is assumed to be the number of engines multiplied with the measured on-board emission rates. In addition some vessels also use auxiliary engines to power generators or bow thrusters, which also add to the total emissions of the ship and can seen by the on-shore measurements but not the on-board measurements. Taking into account all ships and all simultaneous observations, the ratio between on-shore and on-board is about 1.3 ± 0.1 (see Figure 10). Additionally, ship M is equipped with a SCRT (selective catalytic reduction) system to reduce the NO_x emissions, which did not always operate.

4.2 Comparison with other studies

The emission behaviour of vessels is usually described and evaluated by emission factors. These emission factors are relative measures, e.g. the amount of emitted NO_x is expressed per amount of burnt fuel or per amount of power generated by the engine. The absolute emission rate of NO_x has to be calculated from the emission factors and additional information about the fuel consumption. For comparison with the emission factors derived in other studies, two fuel consumption scenarios are considered. In the first scenario, a fuel consumption of 108 $\mathrm{kg\,h^{-1}}$ is assumed, which describes the fuel consumption of a ship with 3200 tons cargo capacity travelling downstream. The second scenario uses a fuel consumption of 162 $\mathrm{kg\,h^{-1}}$, which describes the fuel consumption of a ship with 3200 tons cargo capacity travelling upstream against the current. Both scenarios are based on the specific fuel consumptions in $\mathrm{kg\,km^{-1}}$, which are 6 $\mathrm{kg\,km^{-1}}$ for ships travelling downstream and 15 $\mathrm{kg\,km^{-1}}$

https://doi.org/10.5194/egusphere-2022-767
Preprint. Discussion started: 16 August 2022

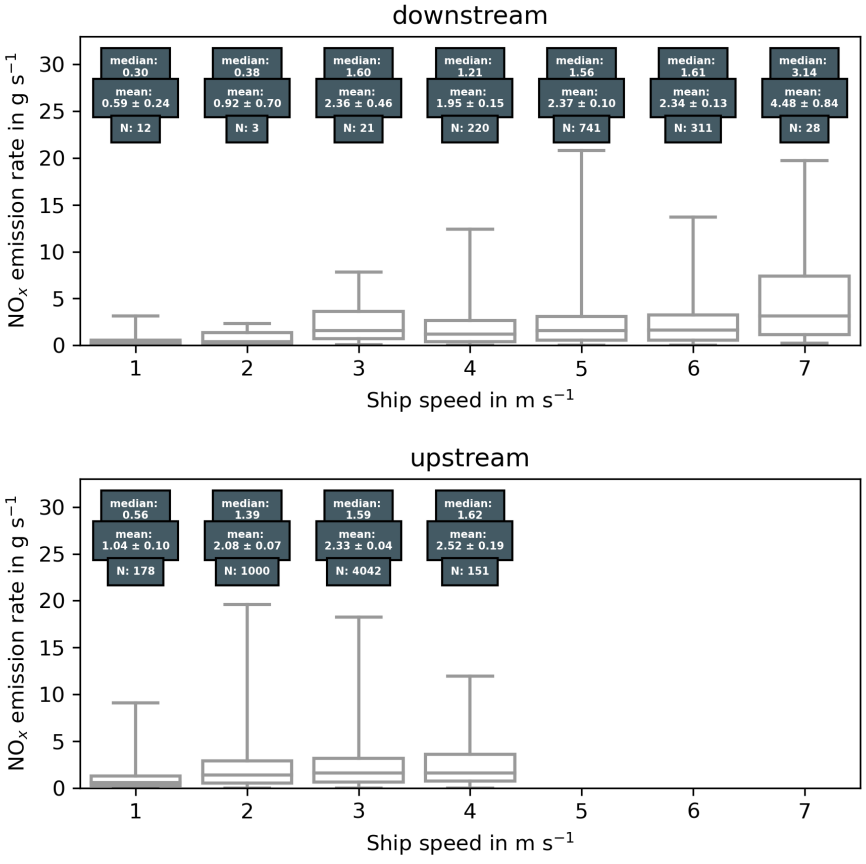

Figure 8. NO_x emission rates for ship class Va and their dependence on the direction of travel and ship speed over ground, derived from data measured at DURH.

for ships travelling upstream (Allekotte et al., 2020). The specific fuel consumptions have been converted to $\mathrm{kg\,h^{-1}}$ using the average speed over ground for ships travelling upstream and downstream, which are 3 and 5 $\mathrm{m\,s^{-1}}$, respectively.

Table 4 shows the comparison of literature values applied to these two scenarios with the emission rates derived in this study. The lower fuel consumption scenario shows absolute NO_x emission rates between 1.17 $\mathrm{g\,s^{-1}}$ to 1.71 $\mathrm{g\,s^{-1}}$. The higher fuel consumption scenario shows emission rates from 1.75 $\mathrm{g\,s^{-1}}$ to 2.57 $\mathrm{g\,s^{-1}}$. In comparison, the mean NO_x emission rates derived in DURH for ships that travel downstream with the most common speed of 5 $\mathrm{m\,s^{-1}}$ are in the range of 2.36 $\mathrm{g\,s^{-1}}$ to 2.53 $\mathrm{g\,s^{-1}}$. For ships travelling upstream with the most common speed over ground of 3 $\mathrm{m\,s^{-1}}$ the NO_x emission rates are 2.17 to 2.36 $\mathrm{g\,s^{-1}}$. Generally, the mean NO_x emission rates fit into the range given by the emission factors of other studies, but are at the upper limit of the given range. At lower speeds, the mean emission rates are also lower (e.g. Figure 8).

Table 5 shows the regulations that are in place for ships built or which had their engine replaced in the specified years. The regulations are defined in $\mathrm{g\,kWh^{-1}}$ and have been converted to $\mathrm{g\,kg^{-1}}$ using a specific fuel consumption of 230 $\mathrm{g\,kWh^{-1}}$

https://doi.org/10.5194/egusphere-2022-767
Preprint. Discussion started: 16 August 2022

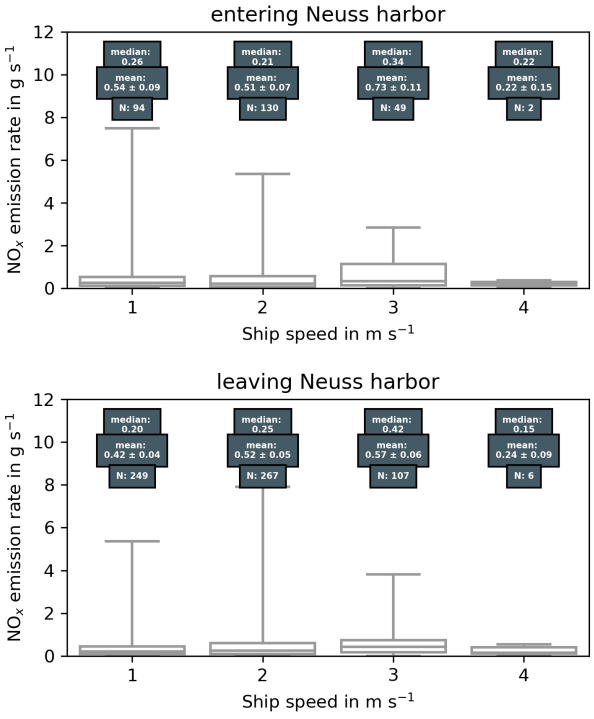

Figure 9. NO_x emission rates for ship class IV and their dependence on the direction of travel and ship speed over ground, derived from data measured at NERH.

(De Vlieger et al., 2004). To interpret the derived NO_x emission rates in the context of these regulations, the limits given in the regulations were converted to $\mathrm{g\,s^{-1}}$ using the 162 $\mathrm{kg\,h^{-1}}$ fuel consumption scenario. These values then can be interpreted as an upper limit for the NO_x emission rates for cases of high fuel consumption. Figure 11 shows the NO_x emission rates derived from the on-shore measurements at DURH for the most common ship classes (VI, Va, Vb and Jowi) as a function of their respective speed over ground. For all ship classes the mean NO_x emission rates for speeds higher than 2 $\mathrm{m\,s^{-1}}$ exceed even the least strict regulation CCNR I of 9.2 $\mathrm{g\,kWh^{-1}}$. For speeds over ground lower than 3 $\mathrm{m\,s^{-1}}$ the mean NO_x emission rates are within the CCNR I limit, but in these cases, the assumed high fuel consumption scenario usually does not apply. When looking at the individual ship passages for the classes IV, Va, Vb and Jowi, approximately 50 % of the derived NO_x emission rates plus their respective uncertainty ($Q_{meas} + \sigma_Q$) are below the CCNR I upper limit, approximately 40 % are below CCNR II and 16 % are below EU RL2016/1629. These results indicate that a large number of old ships with unregulated engines are still in operation.

Kurtenbach et al. (2016) reported emission factors of 20 to 161 $\mathrm{g\,kg^{-1}}$ with an average of 52 $\pm$ 3 $\mathrm{g\,kg^{-1}}$, while Kattner (2019) derived a mean emission factor of 41 $\pm$ 28 $\mathrm{g\,kg^{-1}}$. In both studies the mean emission factor is above the limits given by the regulations, but also here individual ships already comply with them.

https://doi.org/10.5194/egusphere-2022-767
Preprint. Discussion started: 16 August 2022

Table 3. Comparison of NO_x emission rates derived from on-shore measurements and on-board measurements for different ships participating in the CLINSH project. Number of engines only includes main engines used for navigation, and on-board measurements were only carried out on one of them. The number of engines used on ship G is not known, but assumed to be one.

Ship	class	No. of engines	on-shore mean	on-shore median	on-shore std	on-board mean	on-board std	n
			$g\,s^{-1}$	$g\,s^{-1}$	$g\,s^{-1}$	$g\,s^{-1}$	$g\,s^{-1}$	
A	III	1	0.84	0.84	0.27	1.23	0.34	2
B	IV	1	0.94	0.40	0.92	0.81	0.32	6
C	IV	1	2.20	1.66	1.29	1.34	0.51	6
D	Va	1	2.12	1.75	0.63	0.73	0.41	3
E	Va	1	0.56	0.56	-	0.42	0.14	1
F	Va	1	2.40	1.55	2.33	2.17	0.67	45
G	Va	?	1.89	1.77	0.71	1.53	0.32	5
H	Va	1	3.65	3.85	2.44	2.47	1.23	4
I	Jowi	1	1.63	1.77	0.88	1.13	0.32	4
J	Jowi	1	2.05	0.30	3.86	0.71	0.41	13
K	Jowi	1	1.58	1.30	1.10	0.92	0.43	14
L	C-U	1	1.43	0.74	1.49	0.35	0.16	7
M* **	III	2	2.15	1.70	2.24	0.65 (1.30)	0.43 (0.86)	13
N*	Va	3	1.73	0.98	1.81	0.61 (1.83)	0.32 (0.96)	9
O*	Jowi	2	1.56	0.75	2.08	0.72 (1.44)	0.39 (0.78)	25
P*	VIb	2	1.44	0.66	1.37	0.83 (1.66)	0.42 (0.84)	17

* Ships M, N, O and P are equipped with more than one main engine used for navigation. It is assumed that the NO_x emission rates for all engines are the same. The total emission rate for all main engines is therefore assumed to be the number of engines multiplied with the measured on-board emission rates, shown in brackets.
** Ship M is equipped with a selective catalytic reduction (SCR) system to reduce the NO_x emissions, which was not always operating.

In addition, it has to be kept in mind that the water level, hull form and propeller configuration can have a significant influence on the power required to navigate a ship, and therefore on the amount of emitted pollutants (Friedhoff et al., 2018). The mean NO_x emission rates presented here are the result of the evaluation of several years and thousands of different ships. It is therefore expected that the mean values are representative for the average ship emissions on the Rhine in Duisburg.

In addition to regulation of new ships and engines, additional technical measures, such as exhaust gas after-treatment can be used to reduce the emissions caused by ship traffic. The capabilities of exhaust gas after-treatment systems has already been discussed in previous studies (e.g., Schweighofer, J. and Blaauw, H., 2009; Kleinebrahm and Bourbon, 2013; Pirjola et al., 2014; Brandt and Busch, 2017; Busch et al., 2020).

4.3 Ideal measurement location

The improved algorithm presented here, has several advantages over the method described in Krause et al. (2021), where a Gaussian-plume-model was used to derive NO_x and SO_2 emission rates from Long-Path DOAS measurements. An in-situ

https://doi.org/10.5194/egusphere-2022-767
Preprint. Discussion started: 16 August 2022

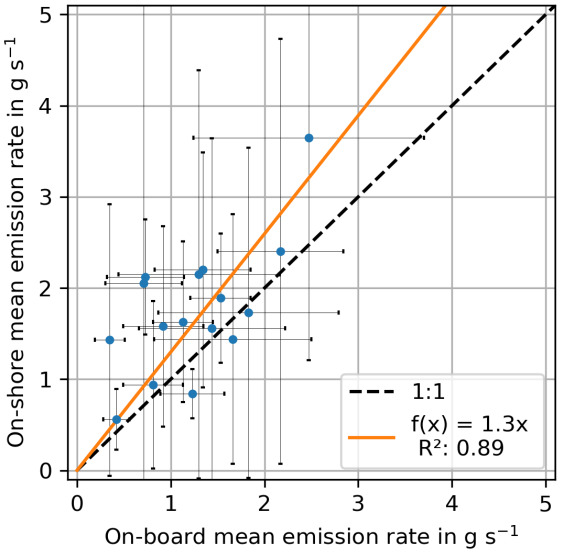

Figure 10. Scatter plot of on-board and on-shore emission rates. Each dot represents the mean value for one ship, errorbars indicate respective standard deviations. For ships with more than one main engine, the number of engines has been taking into account for the on-board emission rates. See also Table 3.

station is easier to model than a remote sensing site, because the concentration is only measured at the location of the station and does not represent the integrated column of an absorber along a light path. The equipment used in this study can be found in standardized air quality measurement stations, facilitating the use of existing stations for ship emission estimates. Only the additional AIS receiver is needed to provide information about the passing vessels. This means that NO_x emission rates can be derived from existing stations with little additional costs. In addition, in-situ measurement stations are able to measure NO and NO_2 simultaneously, so that NO_x can be measured directly and has not to be inferred from NO_2 observations as in Krause et al. (2021).

The measurement stations in DURH and NERH were both suitable locations to derive emission rates from passing vessels under real ship driving conditions. However, their locations are not ideal and increase the difficulty when applying the algorithm to the measurement data. At the time of the installation of the measurement sites, the derivation of on-shore emission factors was not the focus of the CLINSH project. Consequently, we consider that optimisation of the position of the measurement can improve the derivation of the emission rates and lower its uncertainty.

Ideally, a measurement station would be located at a section of a river where there are no confluences. This helps in analysing the derived emission rates, as it is easier to distinguish between ships travelling upstream and downstream. Also it removes possible special manoeuvres carried out by the ships trying to enter or leave a confluence. Further, the measurement station should be located at a straight river section, preferably with the main wind direction orthogonal to the river. This decreases the

https://doi.org/10.5194/egusphere-2022-767
Preprint. Discussion started: 16 August 2022

Table 4. Comparison of the derived NO_x emission rates (ER) in $g\,s^{-1}$ with the emission factors (EF) in $kg\,h^{-1}$ derived from other studies. To calculate the emission rate from the emission factors, two fuel consumption scenarios are evaluated. Both scenarios are based on specific fuel consumption values for ships with a cargo capacity of 3200 tons (approximately class Va and Vb). First a fuel consumption of 108 $kg\,h^{-1}$ is assumed for ships that travel downstream, second a fuel consumption of 162 $kg\,h^{-1}$ is assumed for ships travelling upstream.

Study	NO_x EF in $g\,kg^{-1}$	NO_x ER in $g\,s^{-1}$	NO_x ER in $g\,s^{-1}$
Fuel consumption		108 $kg\,h^{-1}$	162 $kg\,h^{-1}$
Trozzi and Vaccaro (1998)	51	1.53	2.30
Kesgin and Vardar (2001)	57	1.71	2.57
Klimont (2002)	51	1.53	2.30
Rohács and Simongáti (2007)	47	1.41	2.12
Schweighofer, J. and Blaauw, H. (2009)	39	1.17	1.75
van der Gon and Hulskotte (2010)	45	1.35	2.03
Diesch et al. (2013)	53	1.59	2.39
Umweltbundesamt (2013)	49	1.47	2.21
Kurtenbach et al. (2016)	54	1.62	2.43
Kattner (2019)	41	1.23	1.85
This study (DURH)		downstream	upstream
Speed over ground		5 $m\,s^{-1}$	3 $m\,s^{-1}$
IV	-	2.36 ± 0.13	2.17 ± 0.05
Va	-	2.37 ± 0.10	2.33 ± 0.04
Vb	-	2.53 ± 0.17	2.35 ± 0.07
Jowi	-	2.26 ± 0.19	2.36 ± 0.08

Table 5. Overview of NO_x emission limits, according to CCNR (EUD, 1998; CCNR, 2020) and EU regulations (EUR, 2016), in both cases given in units of $g\,kWh^{-1}$. For comparison these have been converted to $g\,kg^{-1}$ using a specific fuel consumption for inland ships of 230 $g\,kWh^{-1}$ (De Vlieger et al., 2004) and eventually to $g\,s^{-1}$ using the 162 $kg\,h^{-1}$ fuel consumption scenario.

Regulation	in effect since	Engine power in kW	NO_x EF in $g\,kWh^{-1}$	NO_x EF in $g\,kg^{-1}$	NO_x ER in $g\,s^{-1}$
CCNR I	2002	P > 130	9.2	39.9	1.80
CCNR II	2007	P > 130	6.0	26.1	1.17
EU RL2016/1629	2019	130 < P < 300	2.1	9.1	0.41
EU RL2016/1629	2019	P > 300	1.8	7.8	0.35

chances of overlapping plumes and therefore increases the chances to identify the source ship. Locations where the wind blows along the river should be avoided, because the plumes of several ships can be mixed and the identification of the source ships can

https://doi.org/10.5194/egusphere-2022-767
Preprint. Discussion started: 16 August 2022

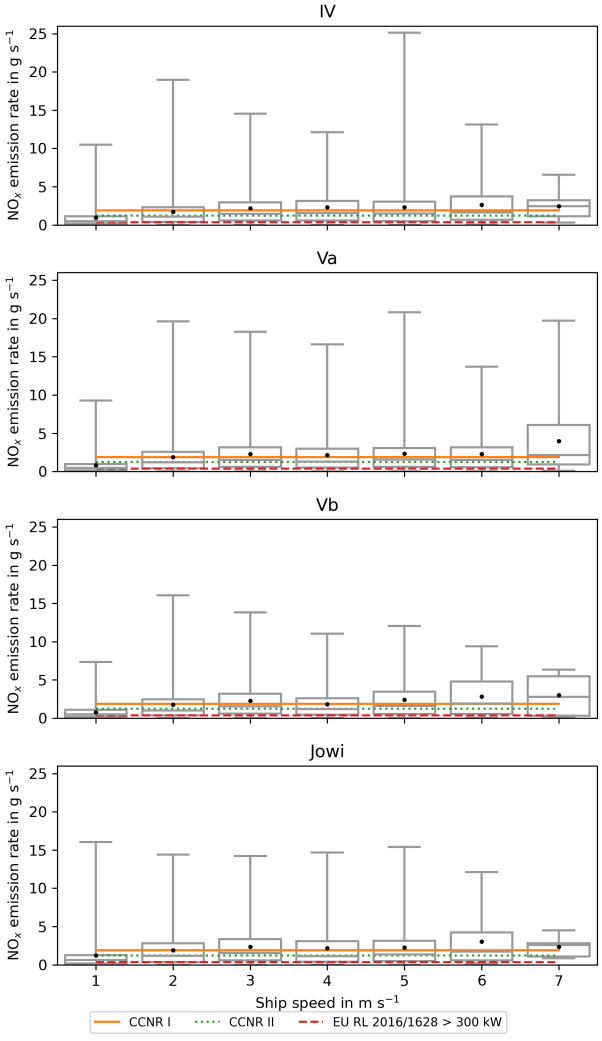

Figure 11. Boxplots of NO_x emission rates for ship classes IV, Va, Vb and Jowi as a function of ship speed over ground, derived from data measured at DURH. Mean value is shown as a black dot, median value as grey line. The limits given by the CCNR I, CCNR II and EU RL2016/1628 regulations were converted from $g\,kWh^{-1}$ to $g\,s^{-1}$ and are shown as lines (see Table 5 for more details).

become impossible, especially when there is high traffic. Locations with point sources of NO_x upwind of the measurement site should also be avoided. These point sources could cause additional peaks, mix with the ship plumes and alter their respective peaks in the measured time series or simply lead to a highly variable background concentration which might be hard to correct. The terrain around the measurement site should be flat and even, so that the surface roughness can be characterized easily. In summary, a simple geometry of the surroundings and a low number of obstacles (i.e. trees, buildings) is beneficial when using the Gaussian-puff-model. In addition, usage of measurements of the current water level would be beneficial because

https://doi.org/10.5194/egusphere-2022-767
Preprint. Discussion started: 16 August 2022

the uncertainty in the height of the emission could be reduced. Incoming solar radiation and cloud cover should ideally be measured at the measurement site, to reduce the uncertainty regarding these parameters.

These suggestions about making emission measurements are not required to the derive the emission rates, as has been shown in this study, but using them will improve the accuracy of future measurements.

5 Conclusions

As part of this study, two standardized in-situ measurement stations have been set up to measure ship emissions on the river Rhine. The first was set up on the river shore in Duisburg to measure the emissions directly at the Rhine, while the second one was installed in the harbour area of Neuss. The measurement stations were established in the period of September to October 2017. The station in Duisburg is still active while that in Neuss made its planned measurements and was dismantled at the end of 2019. For both stations it was possible to identify peaks in the measured NO_x time series and find the corresponding source ships. A new method to derive absolute emission rates (in $\mathrm{g\,s^{-1}}$) from these peaks was developed and successfully applied to the data. Within the algorithm, each individual ship passage is modelled by a Gaussian-puff-model and the modelled concentration at the measurement site is compared to the measured concentration to calculate the emission rate. The modelled concentrations are quality controlled for non-physical results, which can occur when the uncertainty of the input parameters used in the Gaussian-puff-model is too high. In Duisburg approximately 32900 peaks have been identified and could be attributed to a source ship and in approximately 23500 cases, quality controlled emission rates were derived. In Neuss, approx. 5500 peaks have been identified and approx. 3200 emission rates were derived. These emission rates were analysed in context of ship class (size), speed over ground and direction of travel (upstream and downstream).

Generally, the emission rates increase with ship size and ship speed, also the emission rates of ships travelling upstream are higher than those of ships travelling downstream, but have the same speed over ground.

The derived emission rates in this study have been compared to emissions rates measured on-board of ships that participated in the project, and generally good agreement between both methods was found. Discrepancies can be explained by the different quantities that are measured. The on-shore measurements represent the sum of all NO_x emissions of the ship, including all auxiliary engines, while the on-board measurements are only carried out on the main engine. For ships which use more than one engine for navigation, the on-board measurements were only realised for one engine and not for all of them. Therefore, the number of engines had to be considered for the comparison of on-shore and on-board measurements.

The emission rates have been compared to emission factors (in $\mathrm{g\,kg^{-1}}$) from other studies, under the assumption of two fuel consumption scenarios, and agree quite well considering the uncertainties.

The mean emission rates for the most common ship classes (IV, Va, Vb and Jowi) at speeds higher than $2\ \mathrm{m\,s^{-1}}$ exceed even the least strict regulations of CCNR I of $9.2\ \mathrm{g\,kWh^{-1}}$. Looking at individual ship passages for these four classes, approximately 50 % comply with CCNR I, 40 % comply with CCNR II and 16 % comply with EU RL2016/1629.

The algorithm mostly relies on input parameters that are routinely measured by standardized air quality stations, only additional information about the passing ships is needed and can be provided by AIS receivers. In contrast to emission factors, the

https://doi.org/10.5194/egusphere-2022-767
Preprint. Discussion started: 16 August 2022

derived emission rates can be directly used in the conjunction with traffic statistics to model the total emissions caused by ship traffic in the area. This enables possible uncertainties, caused by the assumptions made to convert relative emission factors to absolute emission rates during the modelling process, to be circumvented. In addition, the emission rates include the emission of all engines on-board the ships and not only of the main engine for each passing vessel.

The emission factors collected in 2017-2021 have already been applied by LANUV for the port areas of Duisburg and Neuss within the framework of CLINSH to calculate shipping-related emissions. It is planned to use this procedure for the future update of the inland waterway vessel emission register of the state of North Rhine-Westphalia for the determination of shipping emissions. The continuously measuring station in Duisburg will remain in operation in the coming years and will be evaluated using the described algorithm.

Code and data availability. The data and code used in this study is available directly from the authors upon request.

Author contributions. KK performed the analysis and wrote the manuscript with input from FW, AR, DB, AB an JPB.

Competing interests. The authors declare that they have no conflict of interest.

Acknowledgements. The research presented in this study was funded in part by the EU Life project CLINSH and by the University of Bremen.

https://doi.org/10.5194/egusphere-2022-767
Preprint. Discussion started: 16 August 2022

References

DIRECTIVE 97/68/EC OF THE EUROPEAN PARLIAMENT AND OF THE COUNCIL of 16 December 1997 on the approximation of the laws of the Member States relating to measures against the emission of gaseous and particulate pollutants from internal combustion engines to bin installed in non-road mobile machinery, OJ, L 059, p. 1, https://eur-lex.europa.eu/legal-content/EN/TXT/PDF/?uri=CELEX:01997L0068-20161006&from=EN, 1998.

REGULATION (EU) 2016/1628 OF THE EUROPEAN PARLIAMENT AND OF THE COUNCIL of 14 September 2016 on requirements relating to gaseous and particulate pollutant emission limits and type-approval for internal combustion engines for non-road mobile machinery, amending Regulations (EU) No 1024/2012 and (EU) No 167/2013, and amending and repealing Directive 97/68/EC, OJ, L 252, p. 53, https://eur-lex.europa.eu/legal-content/EN/TXT/?uri=CELEX:02016R1628-20210630, 2016.

Alföldy, B., Lööv, J. B., Lagler, F., Mellqvist, J., Berg, N., Beecken, J., Weststrate, H., Duyzer, J., Bencs, L., Horemans, B., Cavalli, F., Putaud, J.-P., Janssens-Maenhout, G., Csordás, A. P., van Grieken, R., Borowiak, A., and Hjorth, J.: Measurements of air pollution emission factors for marine transportation in SECA, Atmospheric Measurement Techniques, 6, 1777–1791, https://doi.org/10.5194/amt-6-1777-2013, 2013.

Allekotte, M., Biemann, K., Heidt, C., Colson, M., and Knörr, W.: Aktualisierung der Modelle TREMOD/TREMOD-MM für die Emissionsberichterstattung 2020 (Berichtsperiode 1990-2018), 2020.

Ausmeel, S., Eriksson, A., Ahlberg, E., and Kristensson, A.: Methods for identifying aged ship plumes and estimating contribution to aerosol exposure downwind of shipping lanes, Atmospheric Measurement Techniques, 12, 4479–4493, https://doi.org/10.5194/amt-12-4479-2019, 2019.

Beecken, J., Mellqvist, J., Salo, K., Ekholm, J., and Jalkanen, J.-P.: Airborne emission measurements of SO_2, NO_2 and particles from individual ships using a sniffer technique, Atmospheric Measurement Techniques, 7, 1957–1968, https://doi.org/10.5194/amt-7-1957-2014, 2014.

Beecken, J., Mellqvist, J., Salo, K., Ekholm, J., Jalkanen, J.-P., Johansson, L., Litvinenko, V., Volodin, K., and Frank-Kamenetsky, D. A.: Emission factors of SO_2, NO_2 and particles from ships in Neva Bay from ground-based and helicopter-borne measurements and AIS-based modeling, Atmospheric Chemistry and Physics, 15, 5229–5241, https://doi.org/10.5194/acp-15-5229-2015, 2015.

Berg, N., Mellqvist, J., Jalkanen, J.-P., and Balzani, J.: Ship emissions of SO_2 and NO_2: DOAS measurements from airborne platforms, Atmospheric Measurement Techniques, 5, 1085–1098, https://doi.org/10.5194/amt-5-1085-2012, 2012.

Brandt, A. and Busch, D.: Emissionen des Containerschiffs "MS Aarburg": Auswirkungen der Nachrüstung mit einer Diesel-Wasser-Emulsionsanlage, vol. 77 of *LANUV-Fachbericht*, Landesamt für Natur, Umwelt und Verbraucherschutz Nordrhein-Westfalen (LANUV), Recklinghausen, 2017.

Busch, D., Brandt, A., Kleinebrahm, M., and Dreger, S.: Emissionsmessungen auf dem Laborschiff „Max Prüss“ nach Ausrüstung mit einem SCRT-System: Ein Beitrag zum Projekt Clean Inland Shipping (CLINSH), vol. 102 of *LANUV-Fachbericht*, Landesamt für Natur Umwelt und Verbraucherschutz Nordrhein-Westfalen (LANUV), Recklinghausen, https://edocs.tib.eu/files/e01fn21/1745705619.pdf, 2020.

CCNR: Rheinschiffsuntersuchungsordnung (RheinSchUO), https://www.ccr-zkr.org/files/documents/reglementRV/rv1de_012022.pdf, 2020.

Celik, S., Drewnick, F., Fachinger, F., Brooks, J., Darbyshire, E., Coe, H., Paris, J.-D., Eger, P. G., Schuladen, J., Tadic, I., Friedrich, N., Dienhart, D., Hottmann, B., Fischer, H., Crowley, J. N., Harder, H., and Borrmann, S.: Influence of vessel characteristics and atmospheric processes on the gas and particle phase of ship emission plumes: in situ measurements in the Mediterranean Sea and around the Arabian Peninsula, Atmospheric Chemistry and Physics, 20, 4713–4734, https://doi.org/10.5194/acp-20-4713-2020, 2020.

https://doi.org/10.5194/egusphere-2022-767
Preprint. Discussion started: 16 August 2022

Cheng, Y., Wang, S., Zhu, J., Guo, Y., Zhang, R., Liu, Y., Zhang, Y., Yu, Q., Ma, W., and Zhou, B.: Surveillance of SO_2 and NO_2 from ship emissions by MAX-DOAS measurements and the implications regarding fuel sulfur content compliance, Atmospheric Chemistry and Physics, 19, 13 611–13 626, https://doi.org/10.5194/acp-19-13611-2019, 2019.

De Vlieger, I., Int Panis, L., Joul, H., and Cornelis, E.: Fuel consumption and CO_2-rates for inland vessels, Urban Transport X, https://doi.org/10.2495/UT040621, 2004.

Diesch, J.-M., Drewnick, F., Klimach, T., and Borrmann, S.: Investigation of gaseous and particulate emissions from various marine vessel types measured on the banks of the Elbe in Northern Germany, Atmospheric Chemistry and Physics, 13, 3603–3618, https://doi.org/10.5194/acp-13-3603-2013, 2013.

DWD Climate Data Center: Historical 10-minute station observations of solar incoming radiation,longwave downward radiation and sunshine duration for Germany, version V1, a.

DWD Climate Data Center: Selected 81 stations, distributed over Germany, in the traditional KL-standard format, version recent, b.

European Conference of Ministers of Transport: RESOLUTION No. 92/2 ON NEW CLASSIFICATION OF INLAND WATERWAYS, https://www.itf-oecd.org/sites/default/files/docs/wat19922e.pdf, 1992.

Eyring, V., Köhler, H. W., van Aardenne, J., and Lauer, A.: Emissions from international shipping: 1. The last 50 years, Journal of Geophysical Research, 110, https://doi.org/10.1029/2004JD005619, 2005.

Friedhoff, B., List, S., Hoyer, K., and Tenzer, M.: Bestimmung des effektiven Propellerzustroms, https://www.bmvi.de/SharedDocs/DE/Anlage/G/bestimmung-effektiver-propellerzustrom.pdf?__blob=publicationFile, 2018.

Jiang, H., Di Peng, Wang, Y., and Fu, M.: Comparison of Inland Ship Emission Results from a Real-World Test and an AIS-Based Model, Atmosphere, 12, 1611, https://doi.org/10.3390/atmos12121611, 2021.

Kattner, L.: Measurements of shipping emissions with in-situ instruments, 2019.

Kattner, L., Mathieu-Üffing, B., Burrows, J. P., Richter, A., Schmolke, S., Seyler, A., and Wittrock, F.: Monitoring compliance with sulfur content regulations of shipping fuel by in situ measurements of ship emissions, Atmospheric Chemistry and Physics, 15, 10 087–10 092, https://doi.org/10.5194/acp-15-10087-2015, 2015.

Kesgin, U. and Vardar, N.: A study on exhaust gas emissions from ships in Turkish Straits, Atmospheric Environment, 35, 1863–1870, https://doi.org/10.1016/S1352-2310(00)00487-8, 2001.

Kleinebrahm, M. and Bourbon, G.-J.: Minderung der Feinstaub-, Ruß- und Stickstoffoxidemissionen auf dem Fahrgastschiff "Jan von Werth" durch Nachrüstung eines SCRT-Systems, vol. 49 of *LANUV-Fachbericht*, LANUV, Recklinghausen, https://doi.org/Martin, 2013.

Klimont, Z.: Modelling emissions of particulate matter in Europe: A framework to estimate reduction potential and control costs ; Forschungsbericht 29943249, 2002.

Krause, K., Wittrock, F., Richter, A., Schmitt, S., Pöhler, D., Weigelt, A., and Burrows, J. P.: Estimation of ship emission rates at a major shipping lane by long-path DOAS measurements, Atmospheric Measurement Techniques, 14, 5791–5807, https://doi.org/10.5194/amt-14-5791-2021, 2021.

Kurtenbach, R., Vaupel, K., Kleffmann, J., Klenk, U., Schmidt, E., and Wiesen, P.: Emissions of NO, NO_2 and PM from inland shipping, Atmospheric Chemistry and Physics, 16, 14 285–14 295, https://doi.org/10.5194/acp-16-14285-2016, 2016.

Moldanová, J., Fridell, E., Popovicheva, O., Demirdjian, B., Tishkova, V., Faccinetto, A., and Focsa, C.: Characterisation of particulate matter and gaseous emissions from a large ship diesel engine, Atmospheric Environment, 43, 2632–2641, https://doi.org/10.1016/j.atmosenv.2009.02.008, 2009.

https://doi.org/10.5194/egusphere-2022-767
Preprint. Discussion started: 16 August 2022

Pirjola, L., Pajunoja, A., Walden, J., Jalkanen, J.-P., Rönkkö, T., Kousa, A., and Koskentalo, T.: Mobile measurements of ship emissions in two harbour areas in Finland, Atmospheric Measurement Techniques, 7, 149–161, https://doi.org/10.5194/amt-7-149-2014, 2014.

Ramacher, M. O. P., Karl, M., Aulinger, A., Bieser, J., Matthias, V., and Quante, M.: The Impact of Emissions from Ships in Ports on Regional and Urban Scale Air Quality, in: Air Pollution Modeling and its Application XXV, edited by Mensink, C. and Kallos, G., Springer Proceedings in Complexity, pp. 309–316, Springer International Publishing, Cham, https://doi.org/10.1007/978-3-319-57645-9_49, 2018.

Ramacher, M. O. P., Matthias, V., Aulinger, A., Quante, M., Bieser, J., and Karl, M.: Contributions of traffic and shipping emissions to city-scale NO_x and PM2.5 exposure in Hamburg, Atmospheric Environment, 237, 117 674, https://doi.org/10.1016/j.atmosenv.2020.117674, 2020.

Rohács, J. and Simongáti, G.: The role of inland waterway navigation in a sustainable transport system, Transport, 22, 148–153, https://doi.org/10.1080/16484142.2007.9638117, 2007.

Schweighofer, J. and Blaauw, H.: FINAL REPORT THE CLEANEST SHIP PROJECT, https://doi.org/10.13140/2.1.4202.8326, 2009.

Seyler, A., Wittrock, F., Kattner, L., Mathieu-Üffing, B., Peters, E., Richter, A., Schmolke, S., and Burrows, J. P.: Monitoring shipping emissions in the German Bight using MAX-DOAS measurements, Atmospheric Chemistry and Physics, 17, 10 997–11 023, https://doi.org/10.5194/acp-17-10997-2017, 2017.

Seyler, A., Meier, A. C., Wittrock, F., Kattner, L., Mathieu-Üffing, B., Peters, E., Richter, A., Ruhtz, T., Schönhardt, A., Schmolke, S., and Burrows, J. P.: Studies of the horizontal inhomogeneities in NO_2 concentrations above a shipping lane using ground-based multi-axis differential optical absorption spectroscopy (MAX-DOAS) measurements and validation with airborne imaging DOAS measurements, Atmospheric Measurement Techniques, 12, 5959–5977, https://doi.org/10.5194/amt-12-5959-2019, 2019.

Tang, L., Ramacher, M. O. P., Moldanová, J., Matthias, V., Karl, M., Johansson, L., Jalkanen, J.-P., Yaramenka, K., Aulinger, A., and Gustafsson, M.: The impact of ship emissions on air quality and human health in the Gothenburg area – Part 1: 2012 emissions, Atmospheric Chemistry and Physics, 20, 7509–7530, https://doi.org/10.5194/acp-20-7509-2020, 2020.

Trozzi, C. and Vaccaro, R.: Methodologies for estimating air pollutant emissions from ships, Technical Report MEET. (Methodologies for Estimating Air Pollutant Emissions from Transport) RF98, 1998.

Umweltbundesamt: Aktualisierung der Emissionsberechnung für die Binnenschifffahrt und Übertragung der Daten in TREMOD, 2013.

van der Gon, H. D. and Hulskotte, J.: Methodologies for estimating shipping emissions in the Netherlands, A documentation of currently used emission factors and related activity data, BOP report, Netherlands Environmental Assessment Agency, 2010.

Walden, J., Pirjola, L., Laurila, T., Hatakka, J., Pettersson, H., Walden, T., Jalkanen, J.-P., Nordlund, H., Truuts, T., Meretoja, M., and Kahma, K. K.: Measurement report: Characterization of uncertainties in fluxes and fuel sulfur content from ship emissions in the Baltic Sea, Atmospheric Chemistry and Physics, 21, 18 175–18 194, https://doi.org/10.5194/acp-21-18175-2021, 2021.

Wang, X., Yi, W., Lv, Z., Deng, F., Zheng, S., Xu, H., Zhao, J., Liu, H., and He, K.: Ship emissions around China under gradually promoted control policies from 2016 to 2019, Atmospheric Chemistry and Physics, 21, 13 835–13 853, https://doi.org/10.5194/acp-21-13835-2021, 2021.

Zenger, A.: Atmosphärische Ausbreitungsmodellierung: Grundlagen und Praxis, Springer, Berlin and Heidelberg, 1998.

Zhou, F., Pan, S., Chen, W., Ni, X., and An, B.: Monitoring of compliance with fuel sulfur content regulations through unmanned aerial vehicle (UAV) measurements of ship emissions, Atmospheric Measurement Techniques, 12, 6113–6124, https://doi.org/10.5194/amt-12-6113-2019, 2019.

https://doi.org/10.5194/egusphere-2022-767
Preprint. Discussion started: 16 August 2022

Zhou, F., Hou, L., Zhong, R., Chen, W., Ni, X., Pan, S., Zhao, M., and An, B.: Monitoring the compliance of sailing ships with fuel sulfur content regulations using unmanned aerial vehicle (UAV) measurements of ship emissions in open water, Atmospheric Measurement Techniques, 13, 4899–4909, https://doi.org/10.5194/amt-13-4899-2020, 2020.